THE FORMATION OF JETS FROM HEMISPHERICAL-LINER WARHEADS

P.C. Chou*, R.D. Ciccarelli*, W.P. Walters**

*Dyna East Corporation; 3132 Market Street; Philadelphia, PA 19104-2855

**US Army Ballistic Research Laboratory; Aberdeen Proving Ground, MD 21005

The formation of jets from hemispherical-liner warheads is studied by computer code simulation and results are compared with that from conical-liner warheads. Two computer codes are used for the simulation, one is the Eulerian code HELP, the other the Lagrangian code EPIC-2. Both point-initiated explosive and surface-initiated implosion cases are considered. It is shown that the formation of hemi charges is quite different from the classical theory of Pugh-Eichelberger-Rostoker.

I. INTRODUCTION

Recently, shaped charges with hemispherical liners have become candidates for various applications. At present, however, there is no adequate jet formation model for these liners.

There is some question as to whether the classical Pugh-Eichelberger-Rostoker Theory [1] can be applied since there appears to be a significant difference between the hemispherical jet formation process and the conical shaped-charge jet formation process. This difference has been noted by Kiwan and Arbuckle [2]. In fact, some authors [3] have refrained from using the term "jet" for the projected material from hemispherical charges.

One of the most useful tools in studying the jet formation process is the two-dimensional computer code. The commonly used ones are Eulerian codes such as HELP [4] and HULL [5]. Eulerian codes have the advantage of being capable of treating the large material deformation associated with the shaped-charge formation process. The Lagrangian codes usually have the advantage of clearly defined material boundaries, and less computation time. In this paper, we shall present an improved version of an existing Lagrangian code, EPIC-2 [6], which can handle the jet formation process satisfactorily. Simulations of hemi-liner formation by the Eulerian code, HELP, and the Lagrangian code, EPIC-2, will be compared.

The eventual goal of the present research project is to develop a jet formation theory, or model, for hemi liners. In the present paper, emphasis will be placed on the study of two-dimensional computer code simulations. A complete formation theory is being formulated and will be presented in the future.

For practical shaped-charges, the detonation wave is usually initiated from a point or along a plane, or from the peripheral of the explosive charge by wave shaping. In order to gain a basic understanding of the hemispherical liner, a spherical imploding detonation wave is more instructive. This basic geometry was studied by Kiwan and Arbuckle [2]. Results of a code simulation of this imploding charge are compared with the point-initiated charge.

In the following sections, the results from HELP and EPIC simulations will be given first. A comparison between point-initiated and surface-initiated charges will follow. The process of hemi formation will then be presented.

II. EULERIAN AND LAGRANGIAN CODE SIMULATIONS

In this section, we compare the results of Eulerian and Lagrangian two-dimensional code simulations for a point-initiated hemispherical charge. The charge simulated is shown in Figure 1. The Eulerian code simulation was made by BRL using the HELP [4] code. The EPIC-2 [6] code was used by Dyna East in the Lagrangian simulation.

The HELP code calculation of this charge has been discussed in detail previously [7] and only some of the results will be presented here. The EPIC-2 simulation was performed recently using a version of the code modified by Dyna East [8]. This version is quite suitable for the calculation of hemispherical liner collapse and jet formation. A brief description of these modifications follows.

Improvements to EPIC-2 Computer Code

To perform these calculations, an improved version [8] of the two-dimensional finite-element code EPIC-2 [6] was used. The improvements include: 1) a revised method of mass-lumping in axisymmetric problems; 2) enhancements to the sliding-line routines; and 3) crossed-triangle gridding. The effects of these modifications have been to make the simulation more accurate, better-behaved, and less prone to breakdown, and to enable the code to handle the large material distortions encountered in hemi-charge formation.

The EPIC-2 code applies a lumped-mass approach to the finite-element method; that is, the mass of each element is assumed to be concentrated, or lumped, at each of its nodes.

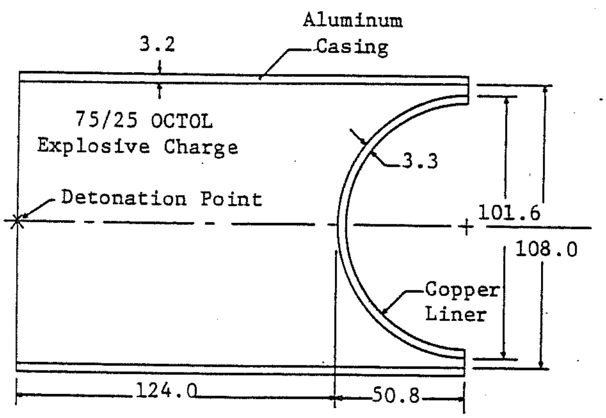

Figure 1. Goemetry of Point-Initiated Hemispherical Charge.

Although less precise than the consistent-mass approach, mass-lumping yields a diagonal mass matrix, with equations of motion that are dynamically uncoupled and, therefore, much easier to integrate. In the origional EPIC-2 code, the mass-lumping was performed by arbitrarily assigning one-third the mass of each triangular element to each of the three corner nodes. It is demonstrated in [8] that, although this is correct for problems of plane geometry, the proper distribution of mass for axisymmetric problems must take into account the radial position of each node. The result is that a node located closer to the axis of symmetry should be assigned a smaller fraction of element mass. In fact, a node located directly on the axis should be assigned only one-quarter the mass of each element attached to it. The nature of the error involved, then, in the original one-third-mass lumping method is the assignment of too much mass to points near the axis, causing them to move more slowly than their neighbors away from the axis. This error was first reported by Johnson [9], who corrected it by introducing a finite-difference formulation near the axis of symmetry. In the version of the code used here, the correction has been made within the finite-element method.

Improvements were also made to the slide-line routines. The major change was the consideration of the forces across the sliding interface during the calculation of the motion of the sliding points. In the original routines, these forces were only imposed after the sliding points had already been moved by the elemental stresses. Other changes to these routines served to more effectively prevent the physically impossible penetrations of one material into another across the sliding planes.

These calculations were performed using a crossed-triangles grid, shown in Figure 2(a), which we have found superior in several aspects to the slashed grid, Figure 2(b). First, the slashed grid has a built-in directional stiffness; under severe shear distortions, the grid can lock itself up, constraining against further shearing. The crossed triangles grid has no preferred direction and allows much more severe distortions. In addition, the slashed grid yields nodal masses that are unbalanced at the boundaries. In Figure 2(b), point A, attached to two elements, has twice the mass of point B, attached to only one element; therefore, with all else equal, point A will move slower than B, giving an incorrect distortion to the grid. Note that in the crossed-triangles grid, the corner points are all connected to two elements, so that the mass is symmetrically distributed.

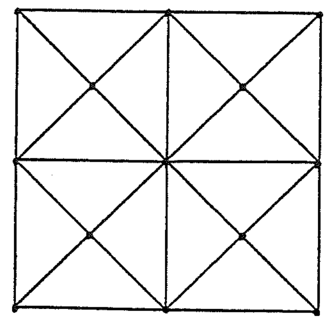

(a) Crossed-Triangles Grid

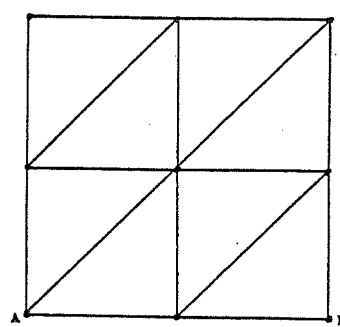

(b) Slashed Grid

Figure 2. Element Grids Used in EPIC-2 Calculations.

Computational Set-Up

Since the EPIC-2 simulation of the charge in Figure 1 has not been previously reported, we will outline the computational set-up. The computational mesh used in our simulation is shown in Figure 3. The previously mentioned crossed-cells are used throughout the problem. The mesh is fine in the region containing the metallic liner. Four rows of crossed-cell triangular elements were placed in the liner as shown in Figure 4. This gave five nodes across the normal thickness of the liner which allowed for direct comparison to the five massless

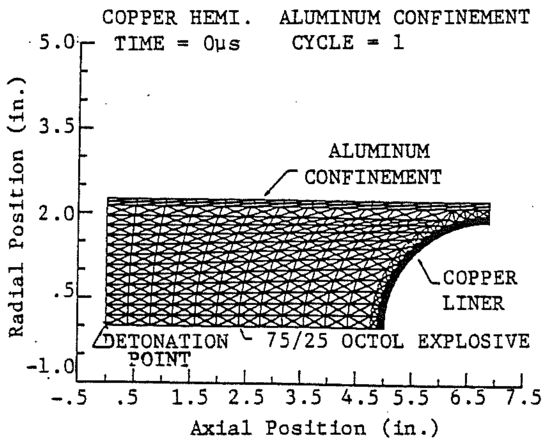

Figure 3. EPIC-2 Code Computational Mesh for Point-Initiated Hemispherical Charge.

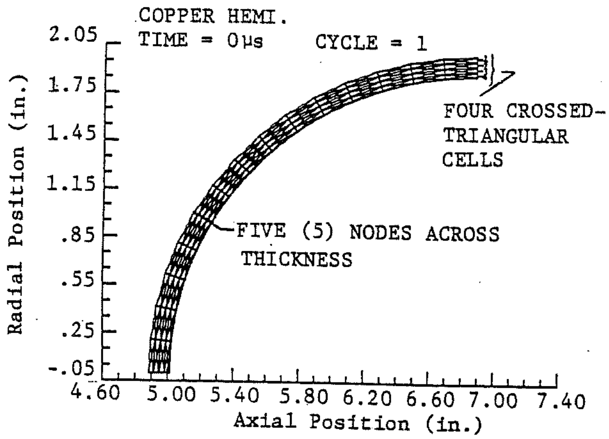

Figure 4. EPIC-2 Code Computational Mesh in Copper Liner.

tracer particles across the thickness in the HELP code simulations [7, 10]. Other studies using the HELP code had concluded that the liner strength was not an important parameter in the simulation of liner collapse and jet formation. Since EPIC-2 does not have the option of setting the liner strength to zero, a low yield strength (0.5 Kbar) was used in the simulation. A Jones-Wilkins-Lee (JWL) [11] equation-of-state was used in the code's explosive burn routine.

Results

The geometries of the jet from both code simulations are compared to the experimental radiographs reported in [7] at both early and later formation times in Figures 5 and 6. The exact scaling factor for the radiographs is not known. As shown in the figures, both codes give good simulations in terms of jet shape in comparison with experiments.

Comparisons of the code calculations of velocity distribution in the jet at two times after explosive detonation are presented in Figures 7 and 8. The velocity distributions from EPIC-2 and HELP are very close. Both codes predict the distribution to be not quite linear, but can be approximated by two straight line segments, or bi-linear. From experiment [7], the tip velocity for this hemispherical charge is 4.43 km/s. The HELP code calculation of tip velocity is 4.39 km/s, which compares very well with experiment. The EPIC-2 code predicts a tip velocity of 4.80 km/s. From past experience with EPIC-2, we have found that its calculated tip velocity is approximately 10% high in comparison to experiment for a series of hemispherical charge configurations.

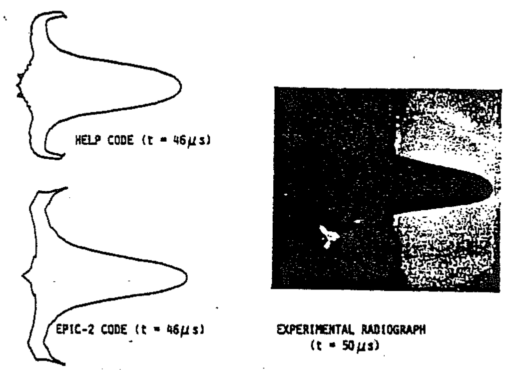

Figure 5. Comparison of Early Jet Formation Shapes from HELP, EPIC-2, and Experiment.

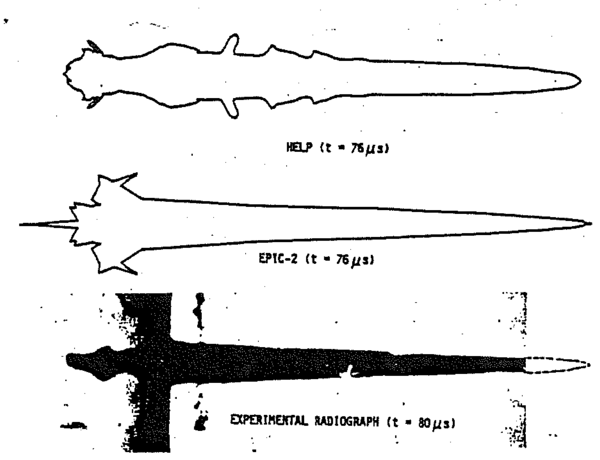

Figure 6. Comparison of Jet Formation Shape from HELP, EPIC-2, and Experiment.

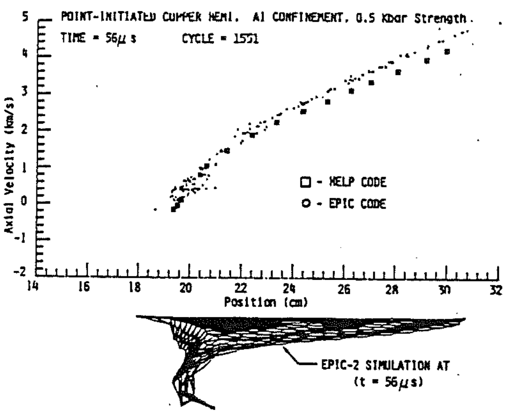

Figure 7. Plot of Axial Velocity vs. Axial Position as Calculated by Both the HELP and EPIC-2 Codes at t = 56μs.

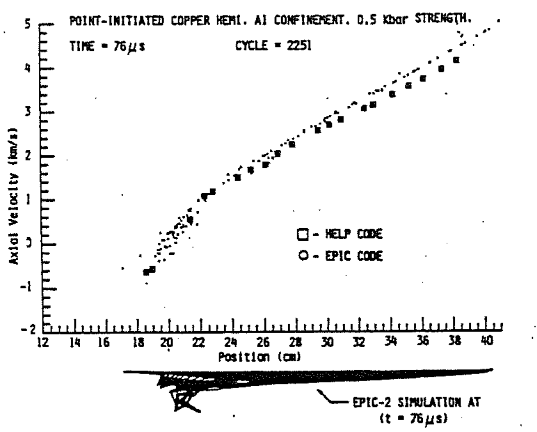

Figure 8. Plot of Axial Velocity vs. Axial Position as Calculated by Both the HELP and EPIC-2 Codes at t = 76μs.

A comparison of the velocity history of liner points located originally along a polar angle of 60° is presented in Figures 9 and 10. From the HELP code simulation, these positions are represented by five massless tracers set across the normal thickness of the liner, [7, 10], number 1 being closest to the free surface. The EPIC-2 plot is representative of five nodes across the normal thickness of the liner, with number 1 on the free surface and number 5 on the explosive-metal surface. Again, we see good agreement between the two codes' calculation of jet velocity.

Based on our analysis of these simulations, both codes show good agreement with experiment. We therefore conclude that it is possible to use a two-dimensional Lagrangian simulation, such as our modified EPIC-2, to model liner collapse and jet formation from a hemispherical charge. EPIC-2, therefore, can be used for two-dimensional calculations in the design synthesis [12] of a hemispherical warhead. This fact is very important since the cost of an EPIC-2 simulation is less than 10% of the cost of an Eulerian code simulation, such as HELP, and the data reduction from the Lagrangian simulation is much easier and less time-consuming.

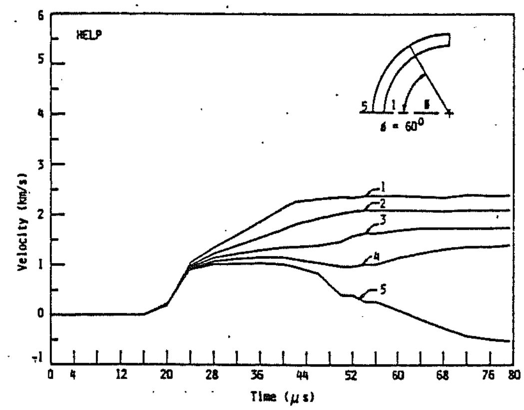

Figure 9. Plot of Velocity vs. Time as Calculated by the HELP Code for the Five Tracer Particles at Original Polar Angle of 60°.

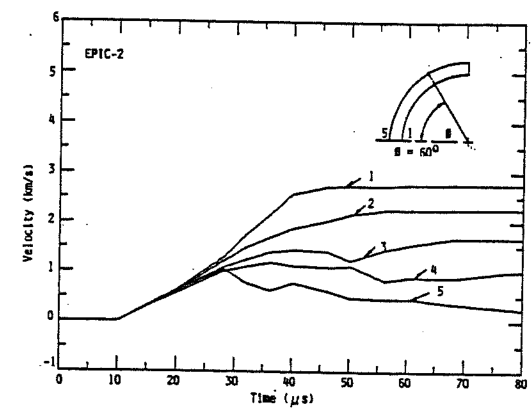

Figure 10. Plot of Velocity vs. Time as Calculated by the EPIC-2 Code for the Five Nodes at Original Polar Angle of 60°.

III. POINT-INITIATED AND SURFACE-INITIATED (IMPLOSION) CHARGES

A comparison was made of HELP code simulations of the point-initiated charge shown in Figure 1 and the surface-initiated or imploding hemispherical charge shown in Figure 11. These charges have the identical metallic liner. The HELP code simulations of these charges have been previously discussed in detail [7, 10]. We will present here some further analysis and a comparison of the liner collapse and subsequent jet formation of the two different charge geometries.

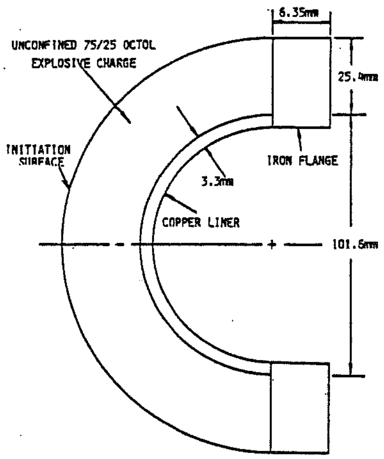

Figure 11. Geometry of Surface-Initiated (Implosion) Hemispherical Charge.

<u>Surface-Initiated Charge</u>

As mentioned in [10], for the imploding hemispherical charge, the jet formation may be divided into three phases, namely; (1) the liner collapse phase, (2) the formation of a high pressure mass phase, and (3) the acceleration into jet phase. An examination of Figures 12-14 gives an indication of the duration of these three phases.

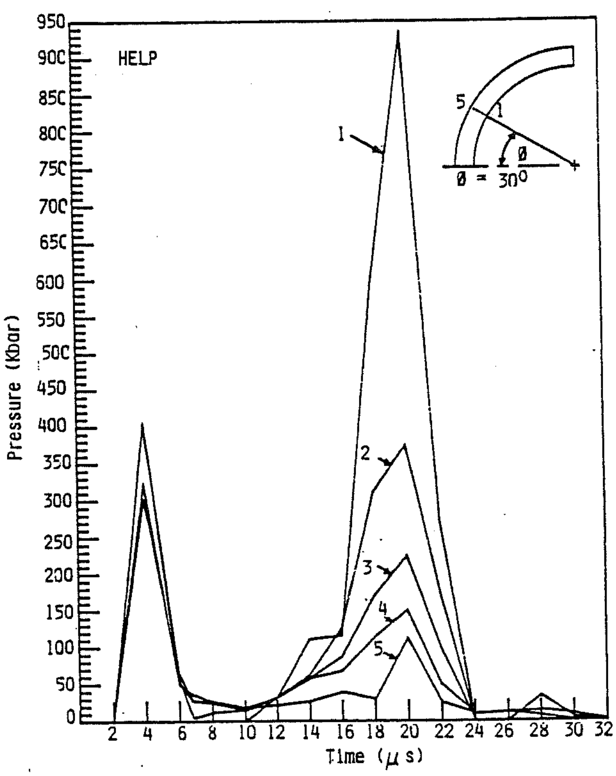

Figure 12. HELP Code Calculation of Pressure vs. Time for Five Tracer Particles at Original Polar Angle of 30° in the Implosive Hemi Liner.

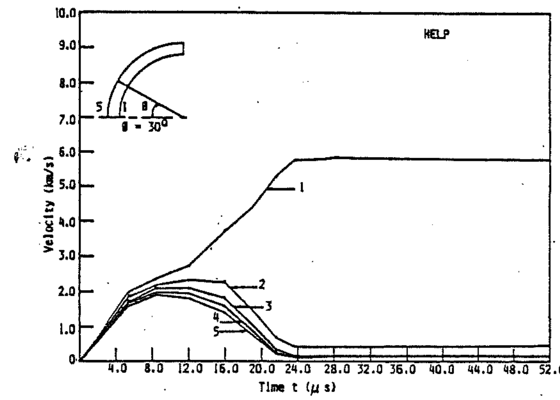

Figure 13. Velocity vs. Time Plots as Calculated by the HELP Code for Five Tracer Particles at Original Polar Angle of 30° in the Implosive Hemispherical Liner.

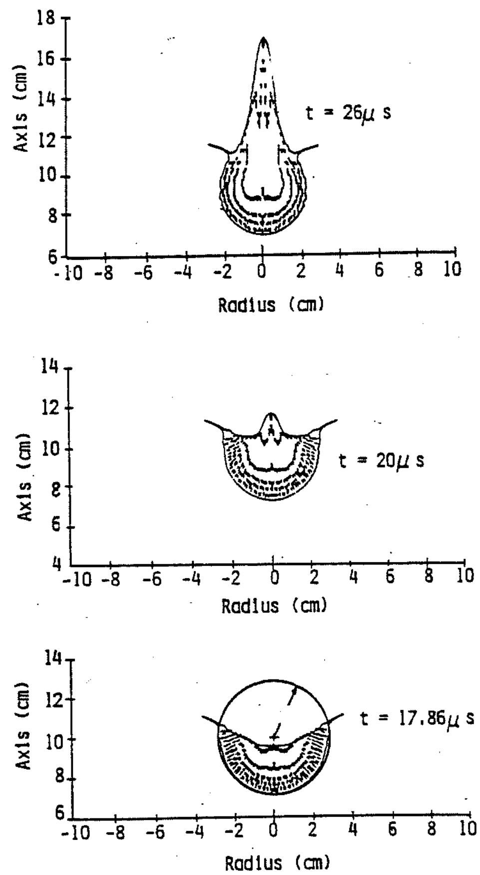

Figure 14. HELP Simulation of Liner Collapse and Jet Formation Showing Velocity Distribution of Tracer Particles at Three Times After Detonation for the Implosive Hemispherical Liner.

For the imploding geometry shown in Figure 11, the detonation wave reaches the liner in about 4μs. As shown in Figure 12, a pressure history curve for tracer particles located at original polar angle, ϕ, of 30°, there is an initial peak pressure at 4μs. The liner collapse phase occurs from 4μs to 10μs. The pressure begins to rise again at 10μs reaching a second peak at 20μs. In this time frame (10μs to 20μs) the high pressure mass is formed. During 20 to 26μs, the acceleration phase occurs. From Figure 12, we can see a drop in pressure in the time frame to essentially zero pressure at 26μs. As indicated in Figure 13, all particles have attained their final velocity of approximately 26μs and maintain an essentially constant velocity motion afterwards.

The process of formation of the high pressure mass can be studied by considering a full spherical shell of the same inside and outside radius as the hemispherical liner under study. Assuming the average radius (one half the sum of outside and inside radii) of the shell has a constant inward velocity of 2.0 km/s, then after 17.4μs, the shell will collapse into a solid sphere of radius 28.8mm. In Figure 14, we can see this sphere superimposed on the collapsing hemispherical liner at 17.86μs. We see that the liner mass is just about filling half of the solid sphere. The equatorial portion of the liner is expanding out due to the rarefaction wave from the free surface. At the center portion of the liner, jetting is about to begin. At 20μs we see the initial jetting, as predicted by the pressure history plot. By 26μs, acceleration has ceased and constant velocity motion is maintained.

Point-Initiated Charge

For the point-initiated charge, shown in Figure 1, the jet formation process differs. The detonation wave reaches the pole of the hemispherical copper liner in approximately 15μs. As stated above, the imploding hemispherical liner experiences two peaks in pressure during jet formation. In the point-initiated case, the liner pressure reaches only one peak, at arrival of the detonation wave as shown in the pressure history plot of Figure 15. The liner in the point-initiated charge experiences a similar collapse phase to that of the imploding charge. Due to the difference in the arrival time of the detonation wave, the starting time of collapse differs for each liner element in the point-initiated case. The detonation wave arrives at the liner pole at 15μs and at the liner equatorial position at approximately 21μs after charge initiation. It is not until t = 46μs that all liner elements attain their final velocity as shown in Figure 16, the velocity history plot for the massless tracers. This is a total of 31μs for all liner elements to collapse and attain final jet velocity compared to 22μs for the imploding case. As seen in Figure 17, the point-initiated liner begins its jetting at approximately 28μs with all liner elements reaching final velocity at 46μs. In the imploding geometry, as is indicated in Figure 14, we see initial jetting at approximately 20μs and all liner acceleration stops at 26μs. This time differential in the jet formation phase results in a large variation in jet tip velocity. The imploding case results in a jet tip velocity of 8.0 km/s compared to a tip velocity of 4.4 km/s in the point-initiated case.

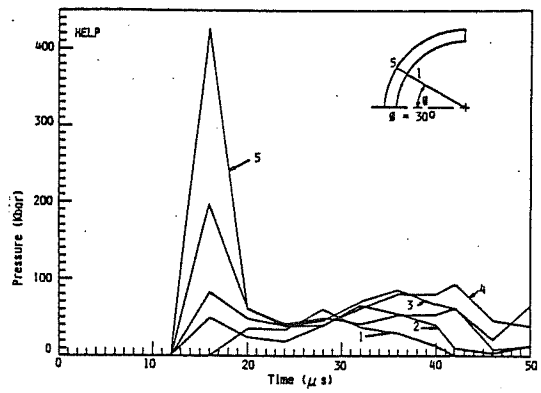

Figure 15. HELP Code Calculation of Pressure vs. Time for Five Tracer Particles at Original Polar Angle of 30° in the Point-Initiated Hemispherical Liner.

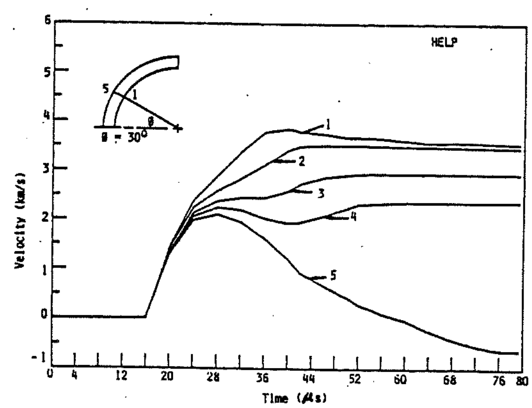

Figure 16. HELP Code Calculation of Velocity vs. Time for Five Tracer Particles at Original Polar Angle of 30° in the Point-Initiated Hemispherical Liner.

IV. HEMI LINER JET FORMATION

According to the classical shaped-charge jet formation theory [1, 13], a ring element of the liner is first accelerated by the explosive to a certain collapse velocity traveling towards the axis of symmetry. When this element is close to the axis of symmetry, it collides upon itself and splits into two elements, a jet and a slug, Relative to the collision point, the jet moves forward and the slug backwards. The following liner element splits the same way, with its jet element trailing the jet element from the previous liner element. The final jet is thus formed by a series of jet elements followed

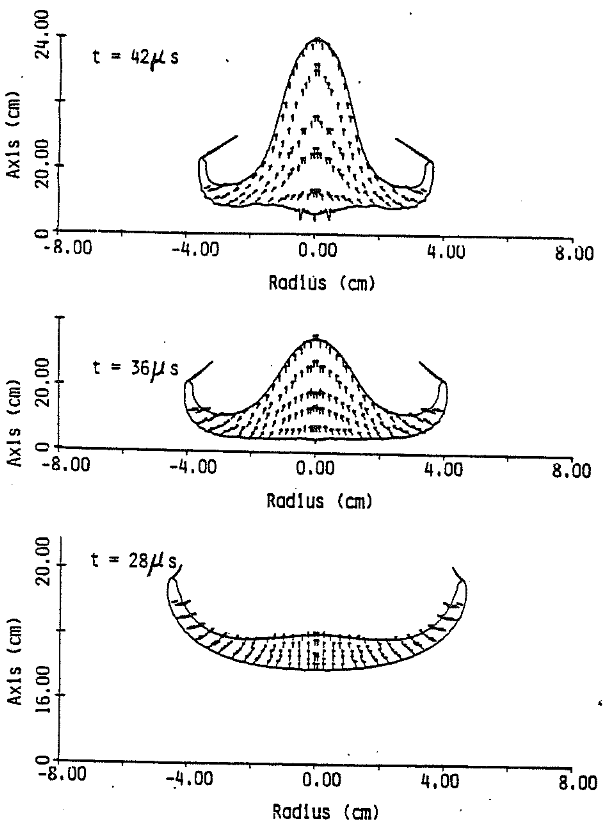

Figure 17. HELP Simulation of Liner Collapse and Jet Formation Showing Velocity Distribution of Tracer Particles at Three Times After Detonation for the Point-Initiated Hemispherical Liner.

by a series of slug elements. Recently, one-dimensional computer codes based on this theory were developed [14, 15]. With empirically determined collapse velocity and collapse angle, these codes have produced satisfactory results, especially for conventional shaped charges with conical liners.

Figure 18 shows the classical theory, as calculated by the DESC code, of the point-initiated hemi-liner charge discussed before. An element in the liner splits into jet and slug elements as shown in the figure.

For the hemi liner charges, the jet formation process is quite different from those of the classical theory. From Figures 14 and 17, it can be seen that the liner first collapses into a high pressure mass. The jet is then formed from this mass. In forming the high pressure mass, all liner elements are combined; it is no longer possible to detect the distinct identity of any liner element in this mass. Later, when the jet is formed, it is formed from this mass that contains all liner elements. It is not possible to say which jet element is from which liner element. Apparently, the formation process of the hemi liner charges is different from that of conical charges, which follow the classical formation process and theory.

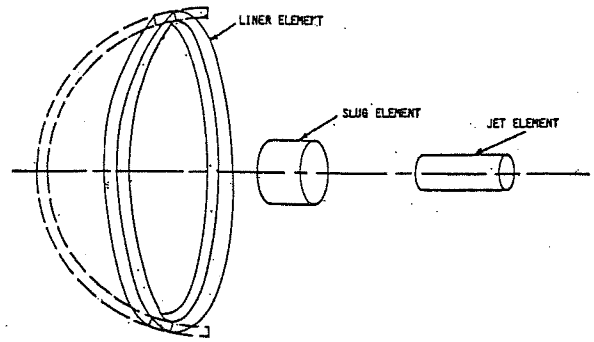

Figure 18. Classical Theory, as Calculated by the DESC Code, of the Point-Initiated Hemispherical Charge.

V. CONCLUDING REMARKS

In this paper, we have pointed out the difference between the formation process of hemi charges and that of conventional conical charges. We are in the process of developing a jet formation theory for hemi-liner charges and hope to present it in the future.

VI. ACKNOWLEDGMENTS

The authors would like to thank Drs. Simcha Miller and William Flis for their assistance with the EPIC code calculations and Mr. Glenn Weaver for performing the HELP code calculations.

VII. REFERENCES

[1] Pugh, E.M.; Eichelberger, R.J.; and Rostoker, N., "Theory of Jet Formation by Charges with Lined Conical Cavities," J. Appl. Phys., Vol. 23, May 1952, pp. 532-536.

[2] Kiwan, A.R. and Arbuckle, A.L., "Study of Liner Collapse, Jet Formation and Characteristics from Implosive Shaped Charge Systems," U.S. Army Ballistics Research Lab Rept. No. 2028, November 1977.

[3] Aseltine, C.L.; Walters, W.P.; Arbuckle, A.L.; and Lacetera, J.E., "Hemispherical Shaped Charges Utilizing Tapered Liners," Proc. 4th Inter. Symp. on Ballistics, Monterey, CA, 17-19 October 1978.

[4] Hageman, L.J. and Walsh, J.M., "HELP, A Multi-Material Eulerian Program for Compressible Fluid and Elastic-Plastic Flows in Two Space Dimensions and Time," Vol. I & II, BRL Cont. Rept. No. 39, May 1971.

[5] Frey, M.A. et al., "The HULL Hydrodynamic Computer Code," U.S. Air Force Weapons Laboratory Rept. No. AFWL-TR-76-183, September 1976.

[6] Johnson, G., "Analysis of Elastic-Plastic Impact Involving Severe Distortions," J. Appl. Mech., V. 98, No. 3, Sept. 1976.

[7] Arbuckle, A.L.; Walters, W.P.; and Aseltine, C.L., "Analysis of Uniform Wall and Tapered Hemispherical Liners with Several Explosive Confinement Geometries," U.S. Army Armament Research & Development Command Tech. Rept. No. ARBRL-TR-02222, March 1980.

[8] Miller, S. and Flis, W., "Improvements to the Two-Dimensional Finite-Element Code EPIC-2," Dyna East Corp. Tech. Rept. No. DE-TR-82-4, September 1982.

[9] Johnson, G., "Recent Developments and Analyses Associated with the EPIC-2 and EPIC-3 Codes," in Advances in Aerospace Structures and Materials, S.S. Wang and W.J. Renton, eds., ASME Publ. No. AD-01, 1981.

[10] Chou, P.C.; Ciccarelli, R.D.; Arbuckle, A.L.; and Walters, W.P., "Jet Formation of an Implosively Loaded Hemispherical Liner," U.S. Army Armament Research & Development Command Cont. Rept. No. ARBRL-CR-00470, September 1981.

[11] Lee, E.; Finger, M.; and Collins, W.; "JWL Equation of State Coefficients for High Explosives," Lawrence Livermore Laboratory Report No. UCID-16189, January 1973.

[12] Carleone, J.; Chou, P.C.; and Simpson, R., "A Synthesis Method for Modern Warhead Design," Proc. of 4th Inter. Symp. on Ballistics, Monterey, CA 17-19 October, 1978.

[13] Carleone, J. and Chou, P.C., "A One-Dimensional Theory to Predict the Strain and Radius of Shaped Charge Jets," Proc. of 1st Inter. Symp. on Ballistics, Orlando, FL, 13-15 November 1974, Sponsored by the ADPA.

[14] Carleone, J.; Chou, P.C.; and Tanzio, C.A., "User's Manual for DESC-1, A One-Dimensional Computer Code to Model Shaped Charge Liner Collapse, Jet Formation, and Jet Properties," Dyna East Corp. Tech. Rept. No. DE-TR-75-4, December 1975.

[15] Harrison, J.T., "BASC, An Analytical Code for Calculating Shaped Charge Properties," Proc. of 6th Inter. Symp. on Ballistics, Orlando, FL, 27-29 October 1981.